Deglycosylation Susceptibility and Base-Pairing Stability of 2′-Deoxyoxanosine in Oligodeoxynucleotide†

Toshinori Suzuki,‡ Yusuke Matsumura,§ Hiroshi Ide,|| Kenji Kanaori,§ Kunihiko Tajima,§ and Keisuke Makino*,‡

Institute of Advanced Energy, Kyoto University, Gokanosho, Uji 611, Japan, Department of Polymer Science and Engineering, Kyoto Institute of Technology, Matsugasaki, Sakyo-ku, Kyoto 606, Japan, and Graduate Department of Gene Science, Faculty of Science, Hiroshima University, 1-3-1 Kagamiyama, Higashi-Hiroshima 739, Japan

Received January 24, 1997; Revised Manuscript Received April 28, 1997⊗

ABSTRACT: We have demonstrated recently that nitrous acid or nitric oxide converts 2′-deoxyguanosine (dGuo) into 2′-deoxyoxanosine (dOxo) [Suzuki, T., Yamaoka, R., Nishi, M., Ide, H., & Makino, K. (1996) *J. Am. Chem. Soc. 118*, 2515−2516]. In the present study, we have measured susceptibility of the *N*-glycosidic bond of dOxo to spontaneous hydrolysis and its base-pairing stability to evaluate the biological significance of dOxo as a new lesion in DNA. When oligodeoxynucleotide d(T_5OT_6) (O = dOxo), isolated from nitrous acid-treated d(T_5GT_6), was incubated at pH 4.0 and 70 °C, hydrolysis of the *N*-glycosidic bond of dOxo occurred with a first-order rate constant. Comparison of the rate constants with those of dGuo and dXao indicates that the *N*-glycosidic bond of dOxo was as stable as that of dGuo in d(T_5GT_6) and hydrolyzed 44-fold more slowly than that of 2′-deoxyxanthosine (dXao), a simultaneously generated damage by nitrous acid and nitric oxide. For the estimation of the base-pairing stability, UV melting curves were measured for the duplexes of d(T_5OT_6)·d(A_6NA_5) (N = A, G, C, and T) at neutral pH. The T_m values obtained were 15.3, 14.1, 19.3, and 16.3 °C for N = A, G, C, and T, respectively, which are much lower than that of the intact duplex containing a G·C pair at the same position [d(T_5GT_6)·d(A_6CA_5), T_m = 32.8 °C] but comparable with those of d(T_5XT_6)·d(A_6NA_5) (X = dXao, T_m = 14.8−22.3 °C). CD spectra of the four duplexes containing dOxo showed preservation of the structure of the intact duplex at low temperature. UV and NMR pH-titration studies indicated the pK_a for the ring-opening and -closing equilibrium to be 9.4, implying that dOxo is in the ring-closed form at physiological pH. This structure appears to be not suitable geometrically for the hydrogen bond formation with a specific counter base, thus causing equally low T_m values for all the counter bases. Consequently, these results imply that dOxo, a novel DNA lesion, may have an important and unique role in mutagenic events in cells.

Oxanosine (Oxo)[1] (5-amino-3-β-(D-ribofuranosyl)-3*H*-imidazo-[4,5-*d*][1,3]oxazin-7-one) has been isolated as a novel antibiotic in 1981 from the culture broth of *Streptomyces capreolus* MG265-CF3 (Shimada et al., 1981) and characterized by X-ray crystallographic study (Nakamura et al., 1981). Oxo manifests wide-range biological effects including *in vitro* cytotoxicity against HeLa cell and antibacterial activity against *Escherichia coli* K-12 and *Proteus mirabilis* IFM OM-9 (Shimada et al., 1981), and induces reversion toward the normal phenotype of K-*ras*-transformed rat kidney cells (Itoh et al., 1989). Its analog, 2′-deoxyoxanosine (dOxo) (Figure 1), has been synthesized from Oxo and found to exhibit stronger antivial and antineoplastic activities than Oxo (Kato et al., 1984).

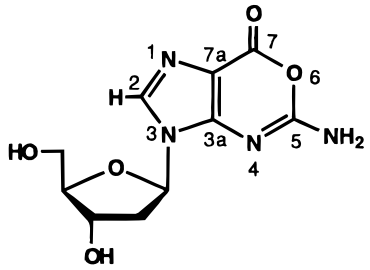

FIGURE 1: Structure of 2′-deoxyoxanosine (dOxo).

Recently, we have shown that dOxo is produced as a major product in the reaction of 2′-deoxyguanosine (dGuo) with nitrous acid (yield, 21.5%), together with 2′-deoxyxanthosine (dXao), a major deamination product (Suzuki et al., 1996). dOxo was also formed in a single-stranded oligodeoxynucleotide (yield, 24.7%) and double-stranded calf thymus DNA (yield, 29.4%). Furthermore, an incubation of an aerated dGuo solution in the presence of nitric oxide (NO) led to dOxo formation at neutral pH.

Many types of cells produce NO through the oxidation pathway of arginine. It was reported that NO concentrations were 100 nM in cerebellar slices after electrical stimulation (Shibuki & Okada, 1991) and 450 nM on the surface of the endothelial cell after chemical stimulation (Malinski & Taha, 1992). NO has many physiological functions, including endothelium-dependent relaxation (Furchgott & Zawadzki, 1980), neurotransmission (Garthwaite et al., 1988), and cell-

† This work was supported partly by Grants-in-Aid for Scientific Research from the Ministry of Education, Science and Culture [to K.M. (08458176) and H.I.].

* Author to whom correspondence should be addressed. Phone: +81−774−38−3517. FAX: +81−774−38−3524. E-mail: kmak@iae.kyoto-u.ac.jp.

‡ Kyoto University.

§ Kyoto Institute of Technology.

|| Hiroshima University.

⊗ Abstract published in *Advance ACS Abstracts,* June 1, 1997.

[1] Abbreviations: dOxo, 2′-deoxyoxanosine; Oxo, oxanosine; Oxa, oxanine (a base moiety of 2′-deoxyoxanosine and oxanosine); dXao, 2′-deoxyxanthosine; Xan, xanthine; dGuo, 2′-deoxyguanosine; Gua, guanine; dThd, 2′-deoxythymidine; dCyd, 2′-deoxycytidine; T_m, melting temperature; ab, abasic site.

S0006-2960(97)00166-9 CCC: $14.00

mediated immune response (Nathan & Hibbs, 1991). There may also be collateral reactions of NO leading to DNA damages in cells. Regarding this, it has been reported that mutations take place in *Salmonella typhimurium* and in human lymphoblastoid cell by NO (Wink et al., 1991; Nguyen et al., 1992). However, these mutations were elucidated only in terms of the formation of deaminated nucleic bases, *i.e.*, uracil, hypoxanthine, and xanthine (Xan). Although studies on biological and genotoxic effects of dOxo formed in DNA in the presence of NO must be important subjects concerning carcinogenesis and apoptosis, there is no information about the chemical and biological properties of dOxo generated in DNA.

In this paper, we describe two biologically important properties of dOxo that are essential to investigate the mutagenesis and carcinogenesis initiated by this damage. One is the rate of hydrolysis of the *N*-glycosidic bond of dOxo, which is discussed in comparison with those obtained for dGuo and dXao. The other is the effect of this lesion on the stability of duplexes, which was determined by measuring the UV melting temperature.

MATERIALS AND METHODS

Materials and Oligodeoxynucleotides. All reagents used for DNA synthesis were obtained from MilliGen/Biosearch, and other chemicals of reagent grade were purchased from Nacalai Tesque (Japan) or Wako Pure Chemicals (Japan). NaOD, DCl, and sodium 3-(trimethylsilyl)propionate-*2,2,3,3-d*$_4$ (TSP-*d*$_4$) used for NMR measurements were purchased from Aldrich. Oligodeoxynucleotides were synthesized on a MilliGen Cyclone Plus automated DNA synthesizer employing standard phosphoramidite chemistry on solid supports. Crude oligodeoxynucleotides were released from the support and deprotected simultaneously in concentrated NH_4OH for 12 h at 55 °C, and subsequently purified by reversed-phase HPLC (RPHPLC). After triethylammonium cation was replaced by Na^+, these samples were desalted with a C18 Sep-Pak cartridge (Waters).

RPHPLC Conditions. An HPLC system consisted of an LC-6A pumping system and a CTO-6A system controller (Shimadzu, Japan). On-line UV spectra were obtained with an SPD-M6A UV−VIS photodiode-array detector (Shimadzu). For RPHPLC, a Hypersil ODS-5 column (4.6 × 150 mm and 5 μm particle size; GL Science, Japan) was used. The eluent was 100 mM triethylammonium acetate (TEAA) buffer (pH 7.0) containing acetonitrile. The gradient of acetonitrile concentration is described in the figure legends. The injected sample volume was 10 μL, the flow rate 1.0 mL/min, and the temperature ambient.

Preparation of dOxo and dXao. 10 mM dGuo was incubated with 100 mM $NaNO_2$ in 3.0 M acetate buffer (pH 3.7) at 37 °C for 2 h. dOxo and dXao were separated from the reaction mixture by RPHPLC with 100 mM TEAA buffer (pH 7.0) as an eluent, subsequently desalted by RPHPLC employing acetonitrile/H_2O (v/v = 5/95), and finally lyophilized.

Molar Extinction Coefficients of Oligodeoxynucleotides. Normal oligodeoxynucleotides used in the present study were d(T_5GT_6) and d(A_6NA_5) (N = A, G, C, T). The molar extinction coefficients of these oligodeoxynucleotides at 260 nm were calculated by the nearest-neighbor method (Cantor & Warshaw, 1970). Values for oligodeoxynucleotides containing dOxo or dXao [d(T_5OT_6) (O = dOxo) and d(T_5XT_6) (X = dXao)] were obtained as follows (Schweitzer & Kool, 1995): As reported previously, the molar extinction coefficients of dOxo and dXao at 260 nm are 5.1×10^3 and 7.8×10^3, respectively (Itoh et al., 1989; Moschel & Keefer, 1989; Suzuki et al., 1996). The individual molar extinction coefficients of all the bases in a given dOxo- or dXao-containing oligomer were summed (*A*) and compared to the sum (*B*) obtained for the corresponding sequence in which dOxo or dXao was replaced by dGuo. The molar extinction coefficient for dOxo- or dXao-containing oligomer was then calculated by multiplying the values derived for the G-containing sequence by the nearest-neighbor parameters, by *A*/*B*. The coefficients obtained for d(T_5OT_6) and d(T_5XT_6) are 9.40×10^4 and 9.69×10^4, respectively.

Enzymatic Digestion of Oligodeoxynucleotides. To identify the nucleosides contained in the HNO_2-treated d(T_5GT_6), the enzymatic digestion was performed. A solution of the oligodeoxynucleotide (0.1 ODU) was incubated in 1.1 mL of Tris-HCl buffer (50 mM, pH 9.0) containing nuclease P1 (Toyobo, Japan) (1 unit), alkaline phosphatase (Toyobo) (12 units), and 10 mM $MgCl_2$ at 37 °C for 4 h. Aliquots of this solution (280 μL) were analyzed by RPHPLC. Oligodeoxynucleotides containing dOxo, dXao, or dGuo showed the expected peak ratio regarding dThd and these nucleosides.

Melting Curves. Absorbance vs temperature melting curves were measured at 260 nm on a U-2000A UV/VIS spectrophotometer (Hitachi, Japan) equipped with an SPR-10 temperature controller (Hitachi). The total strand concentration of the samples was 10 μM in 100 mM potassium phosphate buffer (pH 7.0). The pairs of oligodeoxynucleotides were premelted at 80 °C, and subsequently annealed to 20 °C at the rate of 0.2 °C/min and then to 3 °C at 1 °C/min. For these annealed samples, the UV absorbance at 260 nm was measured with the temperature increase from 3 °C to 80 °C at 1 °C/min. The T_m values were determined by obtaining the first derivation of the melting curves.

Circular Dichroism Spectra. The spectropolarimeter used was J-720 (JASCO, Japan) interfaced with a microcomputer and equipped with an RTE-100 temperature controller (NESLAB). All CD spectra were recorded from 350 to 210 nm at 5 °C with a scan speed of 100 nm/min in a jacketed cylindrical cuvette with a path length of 10 mm. The cuvette-holding chamber was flushed with a constant stream of dry N_2 gas to avoid moisture condensation on the cuvette exterior. The total strand concentration of the samples was 10 μM in 100 mM potassium phosphate buffer (pH 7.0). All the CD data were accumulated 16 times and processed through the noise reduction program.

pH Titration of dOxo. pH-titrated UV spectra were obtained on a DU-86 spectrophotometer (Beckman) at room temperature. 0.1 mM dOxo was dissolved in 10 mL of H_2O. For the pH adjustment, concentrated HCl or NaOH was added to the dOxo solution. Also NMR pH titration was carried out at 30 °C based on the ^{13}C and ^1H resonance. A Bruker ARX-500 NMR spectrometer was employed. dOxo (2 mg) was dissolved in 400 μL of 99.8% D_2O. The pH adjustment was conducted by concentrated DCl or NaOD. The chemical shifts (in ppm) were referenced to TSP-*d*$_4$ as an internal standard. For both UV and NMR measurements, pH values of the samples were monitored using a small-

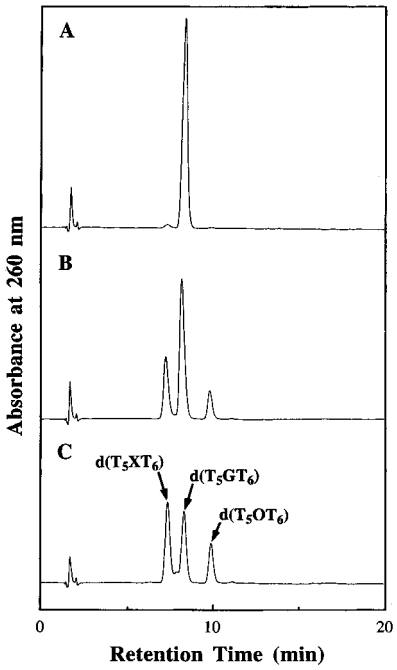

FIGURE 2: RPHPLC of d(T_5GT_6) (10 mM) which was incubated in the presence of HNO_2 (100 mM) in acetate buffer (3.0 M, pH 3.7) at 37 °C for (A) 0, (B) 2, and (C) 5 h. Chromatographic conditions: column, Hypersil ODS-5; sample size, 10 μL; flow rate, 1.0 mL/min; eluent, 100 mM triethylammonium acetate (pH 7.0); gradient (CH_3CN), 11.5% (0 min)−15.0% (linear, 20 min); temperature, ambient; detection, 260 nm. The peak identification is indicated in panel C.

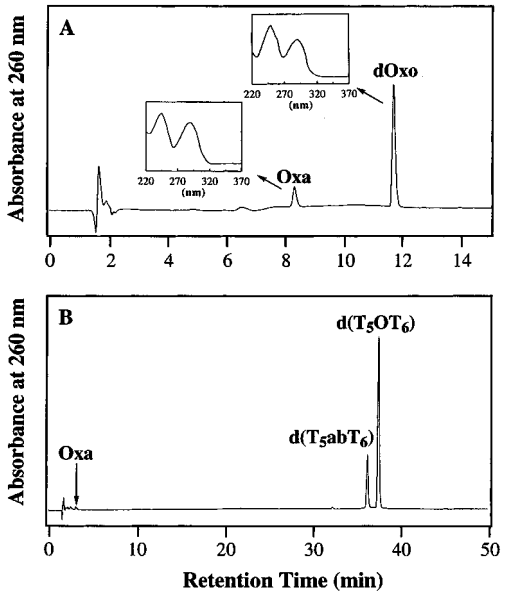

FIGURE 3: (A) RPHPLC profile for dOxo (0.05 mM) incubated in 100 mM acetate buffer (pH 4.0) for 4 h at 70 °C. Photodiode array detection was employed, and the UV spectra obtained for each peak are shown in the insets. (B) RPHPLC profile for the reaction mixtures of d(T_5OT_6) incubated in 100 mM acetate buffer (pH 4.0) for 4 h at 70 °C. Chromatographic conditions were the same as in Figure 2 except that the linear CH_3CN gradient was 0% (0 min)−20.0% (20 min) for panel A and 5.0% (0 min)−15.0% (50 min) for panel B, respectively.

diameter pH probe (Horiba, Japan). The pH values for NMR samples in D_2O are a direct reading of the pH meter which was standardized with H_2O buffer solutions.

RESULTS

Preparation of Oligodeoxynucleotides. Among four normal nucleoside units, only 2′-deoxythymidine (dThd) contains the base without an amino group and therefore does not react with nitrous acid. To introduce dOxo into an oligodeoxynucleotide, this unique property of dThd was used. 10 mM d(T_5GT_6) was incubated in the presence of 100 mM $NaNO_2$ in acetate buffer (3.0 M, pH 3.7) at 37 °C and analyzed by RPHPLC. The chromatograms obtained at the reaction times of 0, 2, and 5 h are shown in Figure 2A,B,C, respectively. The peaks due to the products increased with increase of the reaction time. The peak of retention time (RT) = 8.0 min is obviously attributed to the starting material, and the first and the third peaks in Figure 2C were fractionated and identified as d(T_5XT_6) and d(T_5OT_6), respectively, by analyzing their nucleoside content by RPHPLC after hydrolysis with nuclease P1 and alkaline phosphatase: The assignment of these peaks is indicated in Figure 2C. The percentage yields for d(T_5XT_6) and d(T_5OT_6) at reaction time 6 h were 35.9% and 18.8%, respectively. Each oligomer was isolated by RPHPLC and then desalted by Sep-Pak to use in the following measurements.

Hydrolysis of the N-Glycosidic Bond. To estimate the stability of the *N*-glycosidic bond linking oxanine (the base moiety of dOxo) and the sugar moiety, 0.05 mM nucleosides (dOxo, dXao, and dGuo) were incubated in 100 mM acetate buffer (pH 4.0) at 70 °C. As the dOxo peak (RT = 11.7 min, λ_{max} = 245 and 286 nm) decreased, a new peak (RT = 8.3 min, λ_{max} = 242 and 286 nm) whose UV spectrum is similar to that of dOxo appeared in the chromatogram. A typical RPHPLC chromatogram obtained for dOxo at the reaction time of 4 h is depicted together with the UV spectra in Figure 3A. This product was fractionated and analyzed by ^1H and ^{13}C NMR spectroscopy: ^1H NMR (500 MHz, DMSO-d_6 at 30 °C) δ (ppm/TMS) 12.57 (br, 1H, NH), 7.62 (s, 1H, H-2), 7.58 (s, 2H, NH_2); ^{13}C NMR (125 MHz, DMSO-d_6 at 30 °C) δ (ppm/TMS) 159.5, 154.2, 153.6, 136.5 (C-2), 110.8; UV λ_{max} 240, 286 nm (pH 1), 241, 286 nm (pH 7), 281 nm (pH 13). Since NMR signals are equivalent with those reported previously for the ring and amino protons of dOxo (Suzuki et al., 1996), the product was identified as oxanine, a base unit of dOxo. Similar experiments were conducted for dGuo and dXao, and released guanine (Gua) and xanthine (Xan) were detected by RPHPLC: Gua and Xan were identified by the agreement of UV spectra and RPHPLC retention times with those of the authentic samples (data not shown). These results indicate that cleavage of the *N*-glycosidic bond of these three nucleosides could be quantitatively monitored by RPHPLC. The time courses of the deglycosylation reaction of these nucleosides are presented in Figure 4A. It is obvious that the deglycosylation process shows first-order kinetics, thus allowing us to evaluate the rate constants for hydrolysis of the *N*-glycosidic bond (k) by the first-order reaction equation. The k values obtained for the three nucleosides are listed in Table 1.

Similar kinetic study was performed for single-stranded oligodeoxynucleotides (0.05 mM) [d(T_5OT_6), d(T_5XT_6), and d(T_5GT_6)]. As in the case for the nucleosides, degradation proceeded as a function of the reaction time, and the released bases were detected by RPHPLC. A typical chromatogram obtained for d(T_5OT_6) with an incubation time of 4 h is shown in Figure 3B. In this chromatogram, two peaks appeared in addition to the parent peak of d(T_5OT_6) (RT =

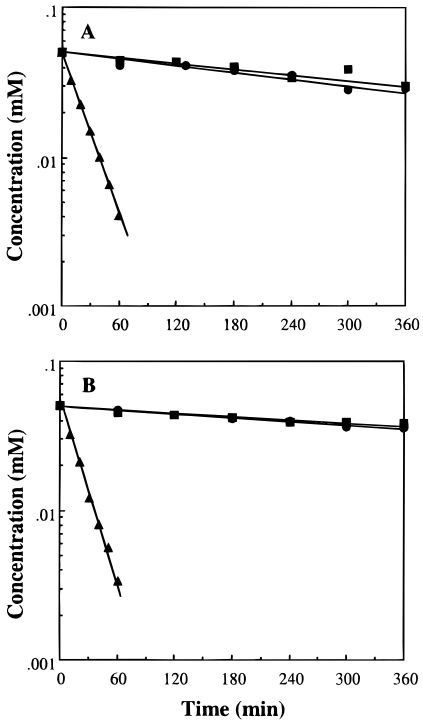

FIGURE 4: (A) Hydrolysis of the *N*-glycosidic bond of dOxo (circles), dXao (triangles), and dGuo (squares) in 100 mM acetate buffer (pH 4.0) at 70 °C. The concentration was calculated by the combination of the RPHPLC peak area and the molar extinction coefficient at 260 nm [ϵ(dOxo) = 5.1 × 10^3 and ϵ(dXao) = 7.8 × 10^3]. (B) Hydrolysis of d(T_5OT_6) (circles), d(T_5XT_6) (triangles), and d(T_5GT_6) (squares) under the same conditions as in panel A. The concentration was calculated by the combination of the RPHPLC peak area and the molar extinction coefficients ϵ[d(T_5OT_6)] = 9.40 × 10^4, ϵ[d(T_5XT_6)] = 9.69 × 10^4, and ϵ[d(T_5GT_6)] = 10.00 × 10^4, respectively.

Table 1: Rate Constants (*k*) for Hydrolysis of the *N*-Glycosidic Bond of dOxo, dGuo, and dXao

substrate	k (×10^{-5} s^{-1})	substrate	k (×10^{-5} s^{-1})
dOxo	2.6	d(T_5OT_6)[a]	1.7
dGuo	2.1	d(T_5GT_6)	1.5
dXao	66.9	d(T_5XT_6)[b]	74.0

[a] O: dOxo. [b] X: dXao.

37.2 min). The first peak (RT = 3.0 min, λ_{max} = 244 and 288 nm) was identified as Oxa by the analogous method applied to dOxo. The second peak (RT = 35.9 min, λ_{max} = 269 nm) was commonly observed in the chromatograms of all the treated oligonucleotides. In the case of d(T_5GT_6), this peak could not be separated from the parent peak due to overlap of the peaks. To identify this hidden peak, *n*-butylamine treatment was performed. By this treatment, the peak of the parent molecule remained at the same retention time, and a new peak (RT = 28.3 min, λ_{max} = 268 nm) emerged simultaneously. Since *n*-butylamine facilitates the cleavage of abasic sites (Tamm et al., 1953; Suzuki et al., 1994), the hidden peak in the d(T_5GT_6) system could be identified as d(T_5abT_6) (ab = abasic site). Using the same treatment, the peaks observed for d(T_5OT_6) and d(T_5XT_6) were also attributed to the same structure. From these results, it is clear that the cleavage of *N*-glycosidic bonds of dGuo, dXao, and dOxo moieties in oligodeoxynucleotides took place under the present reaction condition. The time courses of the deglycosylation for the oligodeoxynucleotides are shown in Figure 4B. Before the quantification, *n*-butylamine

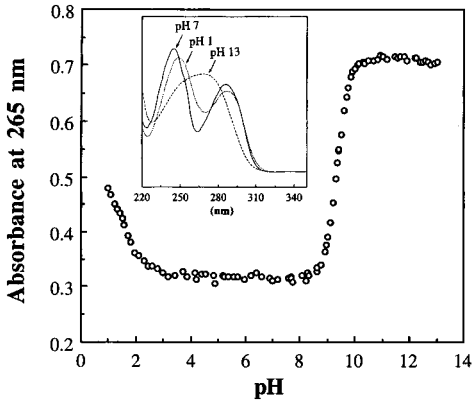

FIGURE 5: pH-dependent change in the absorbance of dOxo at 265 nm. The inset shows typical UV spectra of dOxo at pH 1, 7, and 13. The sample concentration was 0.1 mM.

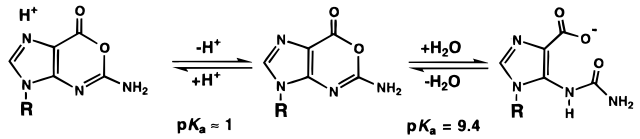

FIGURE 6: Acid−base equilibria for dOxo.

treatment was performed for d(T_5GT_6) to eliminate the overlapping d(T_5abT_6) peak. The *k* values obtained for the oligodeoxynucleotides are summarized in Table 1.

Acid−Base Equilibria of dOxo. Since Oxa contains a lactone structure, dOxo (Figure 1) seems to be subjected to ring opening−closing acid−base equilibria. If this is the case, these equilibria can be monitored by changing the pH. The UV spectra of dOxo exhibited the marked changes with pH (Figure 5, inset) indicative of acid−base equilibria. The UV titration curve was obtained at 265 nm and depicted in Figure 5. The pK_a for the ring opening−closing equilibria was estimated to be 9.4. Taking into account the acid−base equilibria reported for natural purine nucleosides, the other equilibria observed at low pH are likely attributable to the protonation of the imidazole ring (Figure 6). The pK_a value is roughly estimated as 1.

For further exploration of this equilibrium, ^{1}H and ^{13}C NMR spectra were obtained at varied pHs. The titration curves for ^{1}H and ^{13}C NMR chemical shifts are depicted in Figure 7A,B, respectively. Both plots indicate that pK_a for the second equilibrium was around 10, which is consistent with the value obtained by UV spectroscopy. The equilibria at low pH were observed around pH = 1 by ^{1}H NMR, although this value could not be double checked by ^{13}C NMR since dOxo decomposed during long ^{13}C NMR measurements below pH 3. The ^{1}H NMR spectrum obtained at pH 10.0 exhibited signals attributable to both the ring-opened and -closed species simultaneously. In the ^{13}C NMR spectrum, the resonance appeared at 174 ppm, which was assigned to the carboxyl group, supporting the ^{1}H NMR data.

T_m Measurements for Duplexes of Oligodeoxynucleotides. To explore the effect of the dOxo lesion on duplex stability, the UV thermal denaturation study was performed for the four duplexes composed of d(T_5OT_6) (O = dOxo) and its counter strand of d(A_6NA_5) (N = A, G, C, and T). The 260 nm absorbance was plotted against the temperature. As references, analogous measurements were also carried out for the duplexes of d(T_5GT_6) and d(T_5XT_6), which were paired with the same counter strands. All 12 duplexes

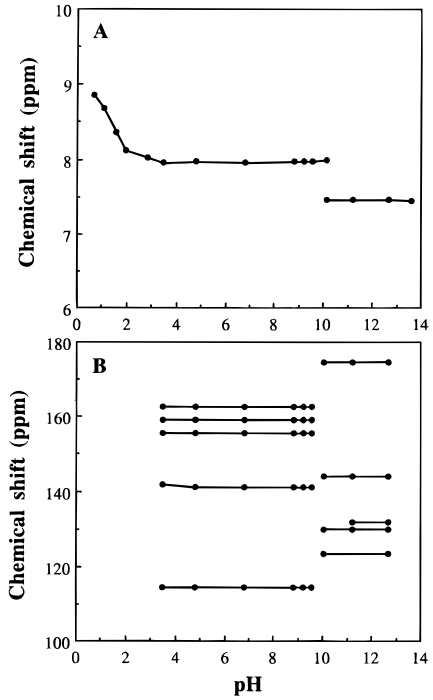

FIGURE 7: pH-dependent change in the chemical shifts of (A) the dOxo H2 proton in the ^{1}H NMR spectra and (B) dOxo ring carbon atoms in the ^{13}C spectra.

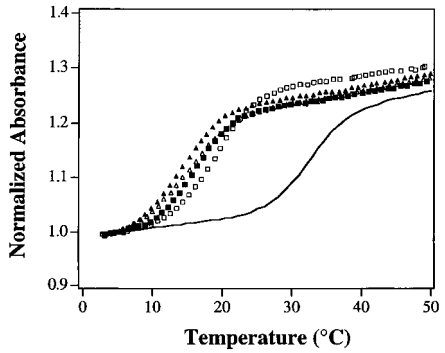

FIGURE 8: Normalized UV thermal denaturation profiles for the duplexes d(T_5OT_6)·d(A_6NA_5) [N = A (open triangles), G (closed triangles), C (open squares), T (closed squares)] and d(T_5GT_6)·d(A_6CA_5) (solid line). The total strand concentration of each sample was 10 μM in 100 mM potassium phosphate buffer (pH 7.0) and detection wavelength at 260 nm. The temperature rise was at 1 °C/min.

Table 2: T_m Values (°C) for Duplexes of d(T_5OT_6), d(T_5GT_6), and d(T_5XT_6) with d(A_6NA_5) (N = A, G, C, and T)

		d(A_{12})	d(A_6GA_5)	d(A_6CA_5)	d(A_6TA_5)
I	d(T_5OT_6)[a]	15.3	14.1	19.3	16.3
II	d(T_5GT_6)	16.8	16.9	32.8	20.4
III	d(T_5XT_6)[b]	17.3	15.6	14.8	22.3

[a] O: dOxo. [b] X: dXao.

showed a single transition in the UV melting curves. The typical UV melting curves for dOxo-containing duplexes d(T_5OT_6)·d(A_6NA_5) are depicted in Figure 8, together with that for the correctly paired duplex d(T_5GT_6)·d(A_6CA_5). The T_m values were determined for all 12 duplexes from the melting curves and are summarized in Table 2. For the d(T_5OT_6) duplexes, the T_m values were in the order of N = C (19.3 °C) > T (16.3 °C) > A (15.3 °C) > G (14.1 °C). These values were significantly low in comparison with that for the correctly paired duplex [d(T_5GT_6)·d(A_6CA_5)] (32.8 °C). To estimate the effect of dOxo on the overall duplex structure, CD measurements were also carried out for the above five duplexes at 5 °C. All the CD spectra were almost identical (Figure 9).

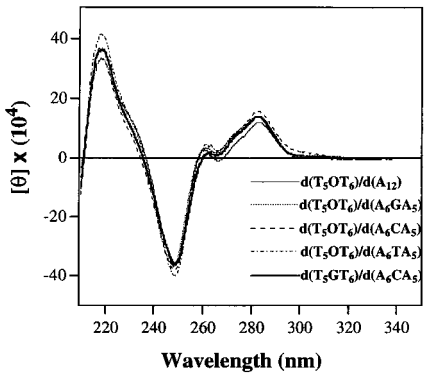

FIGURE 9: CD spectra obtained for the duplexes d(T_5OT_6)·d(A_6NA_5) and d(T_5GT_6)·d(A_6CA_5), at 5 °C. The total strand concentration of each sample was 10 μM in 100 mM potassium phosphate buffer (pH 7.0). All CD data were accumulated 16 times and processed through the noise reduction program.

DISCUSSION

Deglycosylation Susceptibility of dOxo. The *N*-glycosidic bond is the most labile bond in DNA under physiological condition. Moreover, the *N*-glycosidic bond of dXao, a major product of HNO_2- or NO-treated dGuo, is particularly susceptible to spontaneous hydrolysis (Moschel & Keefer, 1989), indicating that a dXao moiety in mammalian cell DNA would be converted to an abasic site within days or weeks at 37 °C by nonenzymatic hydrolysis (Lindahl, 1993). As summarized in Table 1, the present quantitative experiment also revealed that the rate constant for the hydrolysis of the *N*-glycosidic bond of dXao in a single-stranded oligodeoxynucleotide is 49-fold larger than that for dGuo which has the most labile *N*-glycosidic bond of the four natural deoxynucleosides. Since no specific repair enzyme for Xan has been identified (Lindahl, 1993), it is possible that dXao releases Xan spontaneously by nonenzymatic hydrolysis, and the resultant abasic sites can be subjected to repair.

On the other hand, we have shown in the present study that the *N*-glycosidic bond of dOxo is as stable as that of dGuo (Table 1). In the hydrolysis of the *N*-glycosidic bond of dOxo, the rate of deglycosylation was similar to that for dGuo and 26 times lower than that for dXao. The rate constant for a dOxo moiety in d(T_5OT_6) was also comparable to that for dGuo in d(T_5GT_6) and 44 times smaller than that for dXao in d(T_5XT_6). It has been estimated that in *E. coli* genome depurinations of dGuo and dAdo occur 0.5 times per cell per generation (Lindahl, 1982). Taking into account these present and previous data, the rate for spontaneous hydrolysis of the *N*-glycosidic bond of dOxo seems to be a similar level *in vivo* to that of a dGuo moiety. It is deduced that in the cell, dOxo moieties formed in DNA would be infrequently released by spontaneous cleavage of the *N*-glycosidic bond and cannot be subjected to the base excision−repair pathway unless a certain DNA glycosylase specific for dOxo exists.

Structure of dOxo at Physiological pH. To understand structural basis of the specific interactions of dOxo with DNA

polymerases, repair enzymes, etc., determination of the dOxo structure under physiological conditions is essential. Also, structural determination would help to explain whether the low T_m values of the duplexes containing dOxo are due to some specific nature of this lesion. Since it is possible that dOxo exists in acid−base equilibria, we have performed pH-dependent spectroscopic studies for a dOxo solution to see if the equilibria shown in Figure 6 are the case. pH-dependent UV spectroscopy indicated two equilibria at pHs ca. 1 and 9.4. The equilibrium observed at ca. pH 1 is likely due to the protonation at the N1 atom of the imidazole ring of dOxo because this spectral change resembles that for the protonation at N7 of a dGuo residue with pK_a = 2.4 (Suzuki et al., 1994). ^{1}H NMR spectroscopy confirmed this protonation (Figure 7A), where the signal of the H2 proton was shifted to low field with pH. The equilibrium with the pK_a of 9.4 was also explored by NMR. The ^{13}C NMR titration curve (Figure 7B) indicated that the resonance characteristic of the carboxyl carbon (174 ppm) appeared above pH 10, indicative of the ring-opening of dOxo around this pH. The data also show large chemical shift changes for the other carbon atoms at pH 10, indicating the marked structural change of this molecule. The H2 proton also resulted in a sharp decrease around pH 10, supporting the UV and ^{13}C NMR data. Since the ^{1}H NMR spectrum at pH 10 exhibited signals attributable to both the ring-opened and -closed species simultaneously, this equilibrium was a rather slow process with respect to the NMR time scale. These ring-opening and -closing reactions were reversible below and above the pK_a. Considering the pK_a of the base unit, dOxo exists in the ring-closed form at physiological pH. This indicates that the low T_m values obtained for the duplex d(T_5OT_6)·d(A_6NA_5) should arise from reduced hydrogen bond forming ability of dOxo with the natural nucleoside.

Base-Pairing Ability of dOxo. Because sequential fidelity mechanisms operate in the replication process, the insertion of mismatched bases by DNA polymerases occurs infrequently. The most likely discrimination principle for the base selection and the exonucleolytic editing is the Watson−Crick structure which was imposed by a polymerase active site geometry and the melting capacity of mismatch DNA, respectively (Echols & Goodman, 1991). However, once a DNA lesion is generated, selection of nucleoside opposite the lesion could be influenced. Since dOxo has been found to be infrequently hydrolyzed spontaneously and remain in DNA, we carried out thermal denaturation studies to see if dOxo forms a stable pair with specific bases. UV melting curves obtained for d(T_5OT_6)·d(A_6NA_5) were compared with those for d(T_5XT_6)·d(A_6NA_5) and d(T_5GT_6)·d(A_6NA_5). T_m values of the duplexes are summarized in Table 2.

The T_m values for the duplexes of d(T_5OT_6)·d(A_6NA_5) were in the range from 14.1 to 19.3 °C (Table 2). These values are much lower than that of d(T_5GT_6)·d(A_6CA_5) containing a correct base pair (T_m = 32.8 °C). The T_m values of the duplexes containing mismatched pairs [d(T_5GT_6)·d(A_6NA_5) (N = A, G, and T)] were comparable with those of d(T_5OT_6)·d(A_6CA_5). In the base selection step of DNA polymerase, G·T mispair is the most common one, with observed frequencies in a range of 10^{-2}−10^{-4} or less (Echols & Goodman, 1991). Therefore, the present UV thermal denaturation study indicates that the extent of the influence of dOxo on the duplex stability is equivalent with that by the mismatched base pair of dGuo in the intact DNA. For

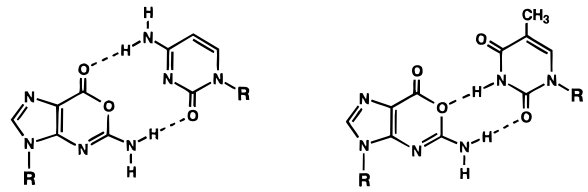

FIGURE 10: Proposed base pairs of dOxo·dCyd and dOxo·dThd.

dXao containing oligomer d(T_5XT_6), the dXao−dThd duplex had the highest T_m (Table 2), which agrees with the previous studies showing that the incorporation rate of dThd triphosphate opposite template dXao was the highest among four natural bases *in vitro* and *in vivo* (Eritja et al., 1986; Kamiya et al., 1992). This consistency may support our present thermal denaturation measurements for dOxo duplexes and further suggest that any base pair between four natural bases and dOxo was unstable. Thus, when the replication takes place in dOxo-containing template, the replication would stop at this site or misincorporation of incorrect nucleotides may occur.

The reason for the low T_m of dOxo-containing duplexes d(T_5OT_6)·d(A_6NA_5) was also explored by CD spectroscopy. All the CD spectra obtained were similar to that of d(T_5GT_6)·d(A_6CA_5) (Figure 9), implying that the base pairs containing dOxo did not induce global structural change. These results suggest that dOxo-containing DNA can be subjected to the replication process. Presumable base-pairing for dOxo based on the hydrogen bonding capacity is illustrated in Figure 10. dOxo having the acceptor−acceptor−donor configuration can form two hydrogen-bondings with either C or T. If this is the case, it is expected that the template dOxo directs incorporation not only of dCTP but also of dTTP.

In conclusion, the *N*-glycosidic bond of dOxo was stable against spontaneous hydrolysis, and dOxo could not form a stable base pair with a specific natural base. The results strongly suggest that the formation of dOxo in DNA is a serious lesion and an enzymatic repair system for dOxo moiety needs to exist in a cell.

REFERENCES

Cantor, C. R., & Warshaw, M. M. (1970) *Biopolymers 9*, 1059−1077.

Echols, H., & Goodman, M. F. (1991) *Annu. Rev. Biochem. 60*, 477−511.

Eritja, R., Horowitz, D. M., Walker, P. A., Ziehler-Martin, J. P., Boosalis, M. S., Goodman, M. F., Itakura, K., & Kaplan, B. E. (1986) *Nucleic Acids Res. 14*, 8135−8153.

Furchgott, R. F., & Zawadzki, J. V. (1980) *Nature 288*, 373−376.

Garthwaite, J., Charles, S. L., & Chess-Williams, R. (1988) *Nature 336*, 385−388.

Itoh, O., Kuroiwa, K., Atsumi, S., Umezawa, K., Takeuchi, T., & Hori, M. (1989) *Cancer Res. 49*, 996−1000.

Kamiya, H., Shimizu, M., Suzuki, M., Inoue, H., & Ohtsuka E. (1992) *Nucleosides Nucleotides 11*, 247−260.

Kato, K., Yagisawa, N., Shimada, N., Hamada, M., Takita, T., Maeda, K., & Umezawa, H. (1984) *J. Antibiot. 37*, 941−942.

Lindahl, T. (1982) *Nucleic Acids Res. Mol. Biol. 22*, 135−192.

Lindahl, T. (1993) *Nature 362*, 709−715.

Malinski, T., & Taha, Z. (1992) *Nature 358*, 676−678.

Moschel, R. C., & Keefer, L. K. (1989) *Tetrahedron Lett. 30*, 1467−1468.

Nakamura, H., Yagisawa, N., Shimada, N., Takita, T., Umezawa, H., & Iitaka, Y. (1981) *J. Antibiot. 34*, 1219−1221.
Nathan, C., & Hibbs, J. B. (1991) *Curr. Opin. Immunol. 3*, 65−70.
Nguyen, T., Brunson, D., Crespi, C. L., Penman, B. W., Wishnok, J. S., & Tannenbaum, S. R. (1992) *Proc. Natl. Acad. Sci. U.S.A. 89*, 3030−3034.
Schweitzer, B. A., & Kool, E. T. (1995) *J. Am. Chem. Soc. 117*, 1863−1872.
Shibuki, K., & Okada, D. (1991) *Nature 349*, 326−328.
Shimada, N., Yagisawa, N., Naganawa, H., Takita, T., Hamada, M., Takeuchi, T., & Umezawa, H. (1981) *J. Antibiot. 34*, 1216−1218.
Suzuki, T., Ohsumi, S., & Makino, K. (1994) *Nucleic Acids Res. 22*, 4997−5003.
Suzuki, T., Yamaoka, R., Nishi, M., Ide, H., & Makino, K. (1996) *J. Am. Chem. Soc. 118*, 2515−2516.
Tamm, C., Shapiro, H. S., Lipshitz, R., & Chargaff, E. (1953) *J. Biol. Chem. 203*, 673−688.
Wink, D. A., Kasprzak, K. S., Maragos, C. M., Elespuru, R. K., Misra, M., Dunams, T. M., Cebula, T. A., Koch, W. H., Andrews, A. W., Allen, J. S., & Keefer, L. K. (1991) *Science 254*, 1001−1003.

BI970166L